Vol. 85, No. 23

Glutamate Excitotoxicity Is Involved in the Induction of Paralysis in Mice after Infection by a Human Coronavirus with a Single Point Mutation in Its Spike Protein[▽]

Elodie Brison, Hélène Jacomy, Marc Desforges, and Pierre J. Talbot*

Laboratory of Neuroimmunovirology, INRS-Institut Armand-Frappier, 531 boulevard des Prairies, Laval, Québec, Canada H7V 1B7

Human coronaviruses (HCoV) are recognized respiratory pathogens, and some strains, including HCoV-OC43, can infect human neuronal and glial cells of the central nervous system (CNS) and activate neuroinflammatory mechanisms. Moreover, HCoV-OC43 is neuroinvasive, neurotropic, and neurovirulent in susceptible mice, where it induces chronic encephalitis. Herein, we show that a single point mutation in the viral spike (S) glycoprotein (Y241H), acquired during viral persistence in human neural cells, led to a hind-limb paralytic disease in infected mice. Inhibition of glutamate excitotoxicity using a 2-amino-3-(5-methyl-3-oxo-1,2-oxazol-4-yl)propranoic acid (AMPA) receptor antagonist (GYKI-52466) improved clinical scores related to the paralysis and motor disabilities in S mutant virus-infected mice, as well as protected the CNS from neuronal dysfunctions, as illustrated by restoration of the phosphorylation state of neurofilaments. Expression of the glial glutamate transporter GLT-1, responsible for glutamate homeostasis, was downregulated following infection, and GYKI-52466 also significantly restored its steady-state expression level. Finally, GYKI-52466 treatment of S mutant virus-infected mice led to reduced microglial activation, which may lead to improvement in the regulation of CNS glutamate homeostasis. Taken together, our results strongly suggest an involvement of excitotoxicity in the paralysis-associated neuropathology induced by an HCoV-OC43 mutant which harbors a single point mutation in its spike protein that is acquired upon persistent virus infection.

Coronaviruses form a family of ubiquitous enveloped RNA viruses that induce respiratory, enteric, and neurological diseases in several species (10). Human coronaviruses (HCoV) are respiratory pathogens responsible for upper and lower respiratory tract infections (49) and for severe acute respiratory syndrome (SARS) (41). Possible involvement of HCoV other than SARS-CoV in more serious human pathologies was recently reviewed (49). Indeed, HCoV have been associated over the years with the development of pneumonia, myocarditis, and meningitis (16, 39) and occasionally acute disseminated encephalitis (54). We have previously demonstrated that HCoV are neuroinvasive in humans, can infect and persist in human neural cells, and can activate glial cells to produce proinflammatory mediators (3–5, 8, 14). Moreover, we have shown that wild-type reference strain HCoV-OC43 has neuroinvasive properties in mice, leading to chronic encephalitis (25) with accompanying disabilities (23). Given that murine coronavirus (mouse hepatitis virus [MHV]), a strain structurally related to HCoV-OC43, can cause neurodegenerative and neuroinflammatory disease in mice and rats (10), we hypothesized that HCoV-OC43 might be associated with neuroinflammatory and/or neurodegenerative human diseases. We have recently reported that a viral variant with four point mutations in its surface spike (S) glycoprotein, acquired during viral persistence in human neural cells (48), led to a drastically

modified virus-induced neuropathology in BALB/c mice, characterized by a multiple sclerosis (MS)-like flaccid paralysis and inflammatory demyelination (24).

Glutamate is the major excitatory neurotransmitter of the central nervous system (CNS) that is involved in several neurophysiological functions. A disruption of its homeostasis can damage neurons, which may eventually lead to cell death (30). This pathological process, designated excitotoxicity, is able to induce degeneration of neural cells following an excessive stimulation of glutamate on its specific ionotropic receptors, 2-amino-3-(5-methyl-3-oxo-1,2-oxazol-4-yl)propranoic acid receptor (AMPAr) and N-methyl-D-aspartic acid receptor (NMDAr) (35). Activation of these receptors results in neural Ca^{2+} influx, which can mediate excitotoxicity by the means of a cascade of events involving free radical production, mitochondrial dysfunction, and the activation of several enzymes involved in normal cell development and function, resulting in damage to the cell membrane, cytoskeleton, and DNA (42). Interestingly, excitotoxicity was reported to be involved in several neurodegenerative diseases, such as Alzheimer's disease and MS, in humans (13). Glutamate reuptake is necessary for the regulation of physiological extracellular glutamate concentrations and is mediated mainly by high-affinity sodium-dependent transporters. At least five different glutamate transporters expressed on neuronal or glial cells (GLT-1, GLAST, EAAC1, EAAT4, and EAAT5) have been well characterized (12), and up to 90% of the total glutamate reuptake in the adult CNS is achieved by the glutamate transporter 1 (GLT-1), expressed mainly on astrocytes (50). In several neurological diseases, disruption of the GLT-1 expression level

---

* Corresponding author. Mailing address: Laboratory of Neuroimmunovirology, INRS-Institut Armand Frappier, 513 boulevard des Prairies, Laval, Québec, Canada H7V 1B7. Phone: (450) 687-5010, ext. 4300. Fax: (450) 686-5501. E-mail: pierre.talbot@iaf.inrs.ca.

was reported to be associated with alteration in glutamate uptake (52).

Glutamate excitotoxicity can damage the cytoskeleton of axons *in vivo*, which may result in the slowing of axonal transport (1, 31). Neurofilaments (NF) are intermediate filaments constituting the neuron cytoskeleton and are involved in the stability of mature axons and the regulation of axonal transport rate. In physiological conditions, the heavy neurofilament proteins (NF-H) are predominantly phosphorylated in axons and nonphosphorylated in neuronal soma and dendrites (19). A shift of this NF phosphorylation state, which is represented by a loss of nonphosphorylated NF in soma and an increase of nonphosphorylated NF in axons, is a sign of neuronal injury (44). Evaluation of the NF phosphorylation state is a useful tool to monitor progressive axonal disabilities, considering that the NF-H protein phosphorylation state has been shown to be a biomarker in neurodegeneration (37). We have already demonstrated that the NF-H phosphorylation state was altered following HCoV-OC43 infection of mice (24).

In the present study, we demonstrate that only a single point mutation (Y241H) in the spike glycoprotein (S) of HCoV-OC43 is sufficient for the induction of motor dysfunctions and a paralytic disease in infected mice. Furthermore, infection of mice with this HCoV-OC43 S mutant induced a significantly strong neuronal dysfunction and a significant decrease in the expression of the glutamate transporter GLT-1 on astrocytes compared to those seen with sham and wild-type-virus infection. Therefore, the virus-induced pathological process appears to be driven by a glutamate excitotoxic mechanism, as blockade of the AMPA receptor attenuated clinical scores (CS) related to the virus-induced paralysis and motor disabilities, partially restored the physiological NF phosphorylation state and GLT-1 expression, and reduced microglial cell activation.

MATERIALS AND METHODS

Viruses. The wild-type reference HCoV-OC43 virus (VR759) was obtained in the 1980s from the American Type Culture Collection (ATCC). The recombinant virus of HCoV-OC43 (rOC/ATCC) was generated using the full-length cDNA clone pBAC-OC43^{FL} and displayed the same phenotypic properties as the wild-type virus, as previously described (47). This recombinant virus was used as the reference control virus for all experiments. We introduced into the spike glycoprotein of HCoV-OC43 one or two point mutations at a time, the D24Y and S83T mutations (corresponding recombinant virus designated rOC/U$_{S24-83}$), the H183R and Y241H mutations (corresponding recombinant virus designated rOC/U$_{S183-241}$), the H183R mutation (corresponding recombinant virus designated rOC/U$_{S183}$), or the Y241H mutation (corresponding recombinant virus designated rOC/U$_{S241}$); mutations were introduced into the full-length cDNA clone pBAC-OC43^{FL} by site-directed mutagenesis using a QuikChange Multi site-directed mutagenesis kit (Stratagene) as recommended by the supplier. Each cDNA clone was transfected into BHK-21 cells, amplified by two passages in the HRT-18 cell line, and sequenced to make sure that only the introduced H183R and/or Y241H mutation was present and that no other mutations appeared.

Survival curves and clinical scores. Female BALB/c mice (Jackson Laboratories) aged 22 days postnatal (dpn) were inoculated by the intracerebral (i.c.) route with $10^{2.5}$ 50% tissue culture infective doses (TCID$_{50}$) of recombinant virus, as previously described (24). Groups of 10 mice infected by each recombinant virus were observed on a daily basis over a period of 21 days postinfection (dpi), and survival and clinical scores related to motor dysfunctions were evaluated. Mice infected with rOC/U$_{S241}$ which presented motor dysfunctions were evaluated and scored according to a scale based on experimental allergic encephalitis (EAE) clinical score (CS) evaluation (0 to 1, normal, with no clinical signs; 1.5 to 2, partial hind-limb paralysis, with a walk close to ground level; 2.5 to 3.5, complete hind-limb paralysis; 4 to 5, moribund state and death).

Infectious-virus assays. For each experimental condition, groups of three infected BALB/c mice were selected randomly every 2 days and dissected to monitor infectious-virus production in brains and spinal cords. Tissues were processed for the presence and quantification of infectious virus by an indirect immunoperoxidase assay as previously described (27).

AMPA receptor antagonist. The specific noncompetitive AMPA receptor antagonist GYKI-52466 [1-(4-aminophenyl)-4-methyl-7,8-methylenedioxy-5H-2,3-benzodiazepine hydrochloride] was obtained from Tocris Bioscience and dissolved in Hanks' balanced salt solution (HBSS; Invitrogen) at a final concentration of 300 μg/ml of HBSS (46). To investigate the effect of treatment with GYKI-52466, two groups of 10 BALB/c mice infected with rOC/ATCC or rOC/U$_{S241}$ were treated intraperitoneally with 3 mg/kg body weight of GYKI-52466 at 12 h postinfection and then twice daily for 3 weeks or with only 100 μl of HBSS (vehicle), to normalize experimental stress conditions, twice daily over a period of 3 weeks. To verify the noncytotoxic effect of the GYKI-52466 solution, sham-infected mice received the same dose of AMPA receptor antagonist. As described in the literature, this pharmacological dose has been reported to have no behavioral effects and to induce neuroprotective actions (20, 40).

Immunohistochemistry. Groups of three BALB/c mice either sham infected or infected with each virus and treated with GYKI-52466 antagonist or vehicle were selected randomly and perfused with a solution of 4% paraformaldehyde at 10 dpi, which corresponds to the peak of viral replication in the spinal cord and the outcome of clinical scores related to paralytic disease. Lumbar segments from spinal cords were cryoprotected in 30% (wt/vol) sucrose, frozen at −20°C, and processed for sets of 8-μm section size with a cryostat (HM 525; Microm). Axonal damage was investigated by assessing the heavy neurofilament (NF-H) phosphorylation state. Tissue sections were incubated with a mouse anti-nonphosphorylated neurofilament monoclonal antibody (MAb) (SMI 311, 1/1,000; Covance), a mouse anti-phosphorylated neurofilament MAb (SMI 312, 1/1,000; Covance), or Mac-2 rat MAb (1/200; ATCC, Cedarlane) for 2 h at room temperature. Tissue sections were then washed and incubated with a secondary anti-mouse or anti-rat biotinylated antibody, before being revealed with an ABC Vectastain kit (Vector Laboratories) as previously described (24). Double staining for astrocytes and glutamate transporter GLT-1 fluorescence was investigated with the primary antibodies polyclonal rabbit anti-glial fibrillary acidic protein (GFAP, 1/1,000; Dako) and goat anti-glutamate transporter GLT-1 (K-16 sc-31582, 1/500; Santa Cruz Biotechnology). Spinal cord sections were blocked with horse serum in phosphate-buffered saline (PBS) 1× for 1 h at room temperature. Following incubation with both primary antibodies for 2 h at room temperature, sections were washed and then incubated in the dark for 2 h at room temperature with the secondary fluorescent antibodies Alexa Fluor 488 anti-rabbit (1/1,000; Invitrogen) and Alexa Fluor 568 anti-goat (1/1,000; Invitrogen). After final PBS 1× washes, tissue sections were incubated for 5 min at room temperature with 4′,6-diamidino-2-phenylindole (DAPI) (1/100; Polysciences Inc.) and then mounted with Immuno-mount and observed under a fluorescence microscope.

Protein extraction and Western blot analysis. Spinal cords from groups of three mice selected randomly were homogenized in radioimmunoprecipitation assay (RIPA) buffer (150 mM NaCl, 50 Mm Tris, pH 7.4, 1% [vol/vol] NP-40, 0.25% [wt/vol] sodium deoxycholate, 1 mM EDTA) supplemented with the protease cocktail inhibitor (catalog no. P8340; Sigma). Lysates were cleared by centrifugation for 5 min at 4°C at 17,000 × *g*, and supernatants were aliquoted and stored at −80°C. A bicinchoninic acid (BCA) protein assay kit (Novagen) was used to determine protein concentration, according to the manufacturer's protocol. Proteins (10 μg per sample) were separated on a Novex NuPage 4-to-12% gradient gel (Invitrogen) and transferred to a polyvinylidene difluoride (PVDF) membrane (Immobilon-P transfer membrane; Millipore) with a Bio-Rad Trans-Blot semidry transfer cell apparatus. Membranes were blocked with Tris-buffered saline containing 1% (vol/vol) Tween (TBS-T) and 5% (wt/vol) nonfat milk at 4°C overnight, and then membranes were incubated with polyclonal rabbit anti-glial fibrillary acidic protein (GFAP, 1/2,000; Dako), guinea pig anti-glutamate transporter GLT-1 MAb (AB1783, 1/1,000; Millipore), Mac-2 rat MAb (1/100; ATCC, Cedarlane), or rabbit anti-GAPDH (glyceraldehyde-3-phosphate dehydrogenase) (1/1,000; Santa Cruz Biotechnology) for 1 h at room temperature. Membranes were washed three times with TBS-T and then incubated for 1 h at room temperature with secondary antibody anti-rabbit (1/1,000; GE Healthcare UK), anti-guinea pig (1/1,000; Millipore), or anti-rat (1/1,000; Kirkegaard & Perry Laboratories) coupled to horseradish peroxidase (HRP); detection was made by chemiluminescence using a Bio-Rad Immun-Star HRP substrate kit. Band detection and semiquantification were made using the GeneSnap software from a Chemi Genius Syngene apparatus. Analysis of variance (ANOVA) tests followed by *post hoc* Tukey's analysis were performed to
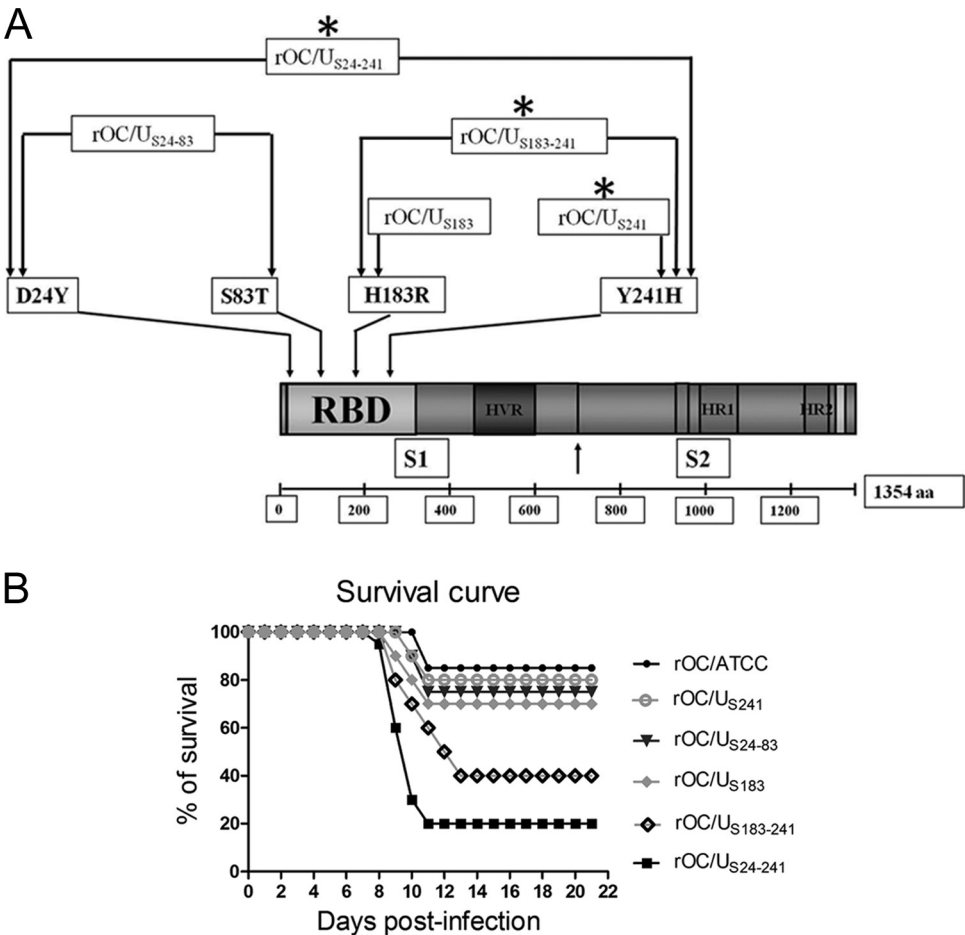
FIG. 1. Schematic representation of the point mutations introduced within the viral spike glycoprotein and associated neurovirulence of the different recombinant viruses in mice. (A) Schematic representation of the main structural domains of the S protein of HCoV-OC43 and the approximate locations of the four point mutations D24Y, S83T, H183R, and Y241H. These mutations were introduced into the viral genome to generate $rOC/U_{S24-241}$ (24). Alternatively, only pairs of mutations were introduced to generate rOC/U_{S24-83} and $rOC/U_{S183-241}$. Finally, one single mutation was introduced at a time to generate rOC/U_{S183} and rOC/U_{S241}. Asterisks indicate recombinant viruses which induced a paralytic disease following infection. RBD, putative cell receptor-binding domain; HVR, hypervariable region; HR, heptad repeat region; aa, amino acids. (B) Survival curves following intracerebral inoculation of the different HCoV-OC43 recombinants harboring various mutations in the S protein compared to that following inoculation with reference rOC/ATCC virus. Whereas infection of mice with the reference virus rOC/ATCC induced 15% mortality, mice infected with $rOC/U_{S24-241}$ showed a mortality rate of 80%. The relative survival rates of mice infected by different viruses containing one, two, or four mutations in the spike protein suggest a synergic effect of these mutations on mortality rate. Results are representative of three independent experiments.

determine the statistical significances in the differences in protein expression between different groups of mice, using SPSS software version 16.0.

RESULTS

BALB/c mice infected with HCoV-OC43 containing the Y241H mutation in the spike glycoprotein (rOC/U_{S241}) develop a hind-limb paralytic disease. We recently showed that a viral variant bearing four point mutations in the spike (S) glycoprotein (D24Y, S83T, H183R, and Y241H), acquired during viral persistence in human neural cells (48), led to a modified virus-induced neuropathology in BALB/c mice compared to that caused by the reference HCoV-OC43 (rOC/ATCC) virus. This modified pathology was characterized by an MS-like flaccid paralysis, with areas of demyelination in the spinal cord, whereas mice infected by HCoV-OC43 (rOC/ATCC) exhibited only encephalitis (24). In order to further

pinpoint the viral molecular determinants responsible for this modulation of virus-induced neuropathogenesis, we generated recombinant viruses that contained two S mutations at a time: D24Y and S83T (designated rOC/U_{S24-83}) or H183R and Y241H (designated $rOC/U_{S183-241}$) (Fig. 1A). Like in infection with virus containing the four mutations described above, infection of BALB/c mice by $rOC/U_{S183-241}$ led to a paralytic disease, with small areas of demyelination in the spinal cord, whereas rOC/U_{S24-83} induced encephalitis like rOC/ATCC. In order to investigate whether only one of the remaining mutations, either H183R or Y241H, was sufficient to induce the paralytic disease in mice, we generated recombinant viruses that harbored only one mutation at a time, either H183R (designated rOC/U_{S183}) or Y241H (designated rOC/U_{S241}) (Fig. 1A). Whereas BALB/c mice infected with rOC/U_{S183} developed an encephalitis similar to what was observed after

rOC/ATCC infection, mice infected with rOC/U_{S241} presented motor dysfunctions and paralytic disease. Neurovirulence of all recombinant viruses was evaluated following intracerebral inoculation of BALB/c mice (Fig. 1B). The survival curves of mice infected by the recombinant viruses bearing one, two, or four point mutations within the viral spike glycoprotein suggested a synergistic effect of these mutations on the mortality rate. Histological examination of infected CNS cells revealed that the primary target cell of the infection by all of these recombinant viruses ($rOC/U_{S183-241}$, rOC/U_{S183}, and rOC/U_{S241}) remained the neurons (data not shown), as previously described for $rOC/U_{S24-241}$ and rOC/ATCC (24). The rOC/U_{S241} recombinant virus was associated with motor dysfunctions in infected mice. Therefore, we conclude that the Y241H single mutation was necessary and sufficient to generate the observed paralytic phenotype and focused the rest of the study on this recombinant virus to evaluate the involvement of this single Y241H mutation in paralytic disease, in comparison to the reference virus rOC/ATCC.

To determine whether the difference in pathology induced by rOC/U_{S241} and the reference virus rOC/ATCC could be related to differences in kinetics of replication in the CNS, brains and spinal cords were harvested and infectious-virus titers were assayed every 2 days for a period of 22 dpi. Even though both viruses replicated to similar extents in the CNS and the highest level of infectious virions were found at 10 dpi in brains as well as in spinal cords, rOC/U_{S241} remained in the spinal cord for a longer period of time than rOC/ATCC. Indeed, infectious rOC/U_{S241} virus was still detectable at 15 dpi, whereas rOC/ATCC infectious virus was never detectable beyond 12 dpi (Fig. 2). Even though viral persistence was not evaluated, we have already reported that viral RNA of wild-type reference HCoV-OC43 (ATCC VR759) (23) and recombinant viruses rOC/ATCC (which has exactly the same genomic sequence as the virus ATCC VR759) and $rOC/U_{S24-241}$ (24) persists in mice for several months postinfection.

AMPA receptor antagonist (GYKI-52466) treatment attenuates mouse motor dysfunctions and severe paralysis induced following infection by rOC/U_{S241}. In order to characterize a possible involvement of excitotoxicity in rOC/U_{S241}-induced hind-limb paralysis, mice infected by rOC/U_{S241} were treated with the AMPA receptor antagonist GYKI-52466 or vehicle (HBSS). GYKI-52466 treatment did not affect the survival rate of mice infected by either rOC/ATCC or rOC/U_{S241} (Fig. 3A), but it attenuated clinical scores related to motor dysfunctions and paralytic disease induced following rOC/U_{S241} infection (Fig. 3B). Indeed, fewer mice presented mild paralysis (CS, 1.5 to 2), and they recovered more rapidly when treated with GYKI-52466, than control vehicle-treated mice. Moreover, whereas 20 to 30% of mice infected by the rOC/U_{S241} virus and treated with vehicle presented severe paralysis (CS, 2.5 to 3.5), only 5 to 10% of the mice treated with GYKI-52466 (with the exception of 12 to 13 dpi) fell into this category (Fig. 3B). Furthermore, recovery was more rapid following treatment with GYKI-52466. The worst symptoms of motor dysfunctions were observed at 10 dpi, and symptoms disappeared totally in the following 6 days of GYKI-52466 treatment, whereas motor disability persisted in vehicle-treated mice. Indeed, as early as 18 dpi, surviving mice infected and treated with AMPA antagonist recovered completely, with no more detectable motor
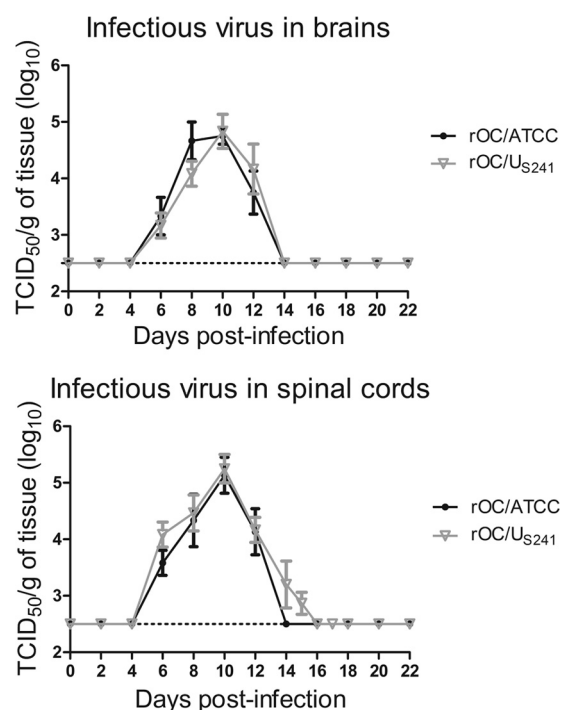
Infectious virus in brains

Infectious virus in spinal cords

FIG. 2. Infectious-virus production measured in the CNS of infected mice. The kinetics of infectious-virus production in brains and spinal cords were evaluated every 2 days for 22 dpi. Both viruses replicated to similar levels, with the same kinetics in brains, and the highest levels of infectious virions were found at 10 dpi in brains as well as in spinal cords. Recombinant virus rOC/U_{S241} was cleared less rapidly from the spinal cord, as infectious virus was repeatedly detected for up to 15 dpi. Results are representative of two independent experiments, and error bars represent standard errors of the means (SEM).

CS. On the other hand, 20% of the infected mice treated with vehicle only still presented severe paralysis (CS, 2.5 to 3.5) at 21 dpi. Viral replication in brains and spinal cords was assessed in mice infected by rOC/U_{S241} or rOC/ATCC and treated with GYKI-52466 or vehicle. For both recombinant viruses, treatment with GYKI-52466 did not modify viral replication (Fig. 3C).

AMPA receptor antagonist treatment reduces neuronal dysfunction in mice infected by rOC/U_{S241}. Spinal cords from mice infected by rOC/U_{S241} or rOC/ATCC and treated with the AMPA receptor antagonist (GYKI-52466) or vehicle were harvested at 10 dpi (time of motor dysfunctions and severe paralysis) to evaluate whether a neuronal alteration associated with excitotoxicity was under way in infected mice. Neuronal dysregulation was investigated by evaluating the axonal neurofilament phosphorylation state. Using SMI 311, an antibody against nonphosphorylated NF-H proteins, we found that infection of mice with rOC/ATCC and rOC/U_{S241} resulted in abnormal loss of soma nonphosphorylated NF-H in the spinal cord gray matter (GM) compared to the result for sham-infected mice. This modification in the phosphorylation state was much more pronounced following infection with rOC/U_{S241} than following infection with rOC/ATCC (Fig. 4, SMI 311 GM). On the other hand, spinal cord white matter (WM) of mice infected with rOC/ATCC and rOC/
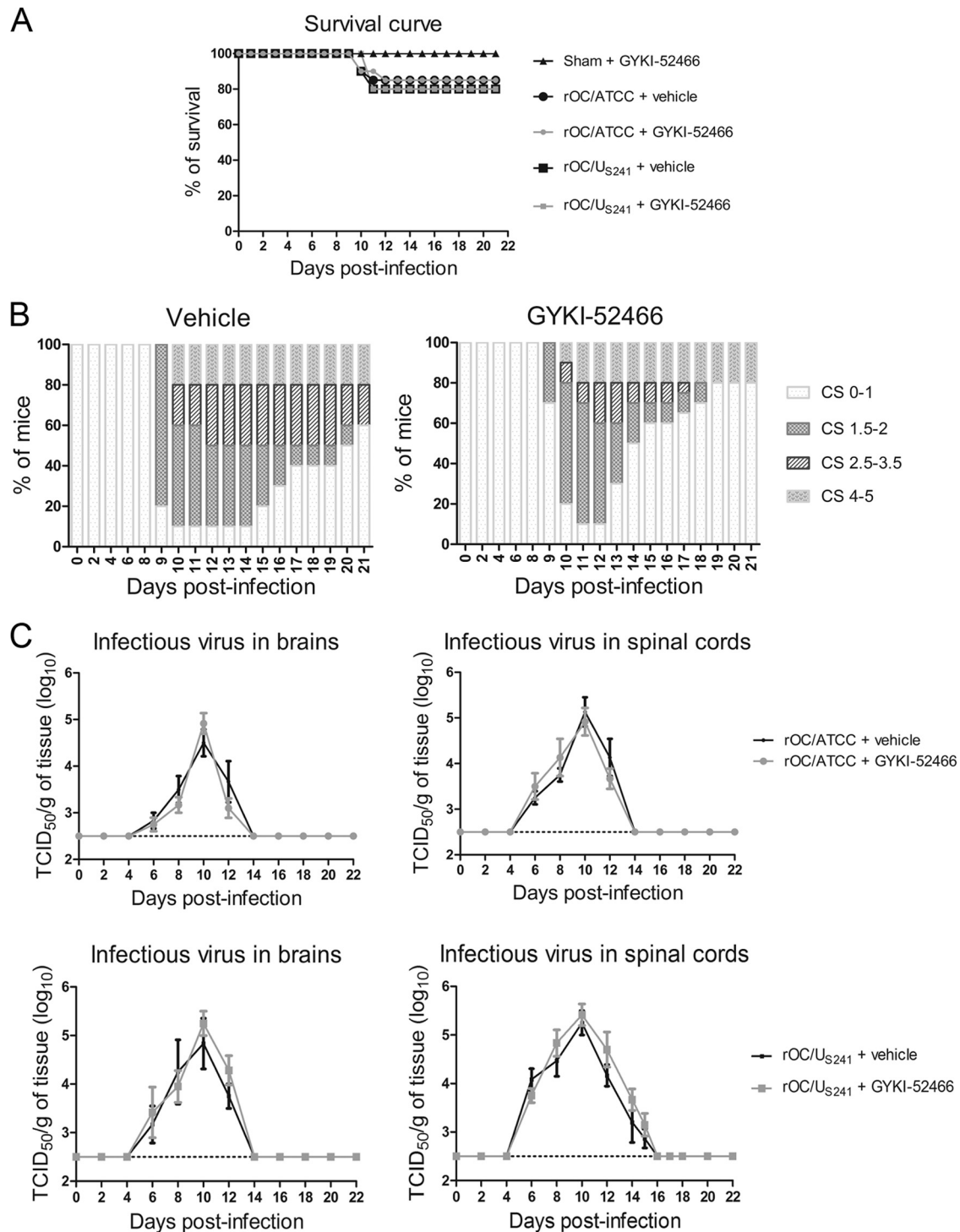
FIG. 3. AMPA receptor antagonist GYKI-52466 treatment attenuates motor dysfunctions in infected mice without modifying neurovirulence or viral replication. (A) Survival curves of mice infected by rOC/U_{S241} or rOC/ATCC and treated with GYKI-52466 or vehicle. GYKI-52466 treatment did not change the rate of survival of mice following infection by either virus. Results with sham-infected mice treated with GYKI-52466 alone illustrated that AMPA treatment was not toxic under the condition used. Results are representative of two independent experiments. (B) Effect of GYKI-52466 treatment on motor clinical scores in mice infected by rOC/U_{S241} and treated with GYKI-52466 or vehicle. GYKI-52466 treatment attenuated clinical scores related to mild (CS, 1.5 to 2) or severe (CS, 2.5 to 3.5) paralysis for mice infected by rOC/U_{S241}, compared to scores for mice treated only with vehicle. Twenty to 30% of mice infected and treated with vehicle presented CS of severe paralysis (CS, 2.5 to 3.5), whereas only 5 to 10% of mice treated with GYKI-52466 fell into this category. The CS of motor dysfunction completely disappeared at 18 dpi in GYKI-52466-treated mice, whereas 20% of mice infected and treated with vehicle only still presented severe paralysis (CS, 2.5 to 3.5) at 21 dpi. Mice that presented mild paralysis (CS, 1.5 to 2) were fewer and recovered more rapidly when treated with GYKI-52466. Results are representative of three independent experiments. (C) Infectious-virus titers in the CNS of mice infected by rOC/U_{S241} or rOC/ATCC and treated with GYKI-52466 or vehicle. For both recombinant viruses, viral replication (kinetics and total amount of infectious virus) was not affected following GYKI-52466 treatment. Results are representative of two independent experiments, and error bars represent SEM.
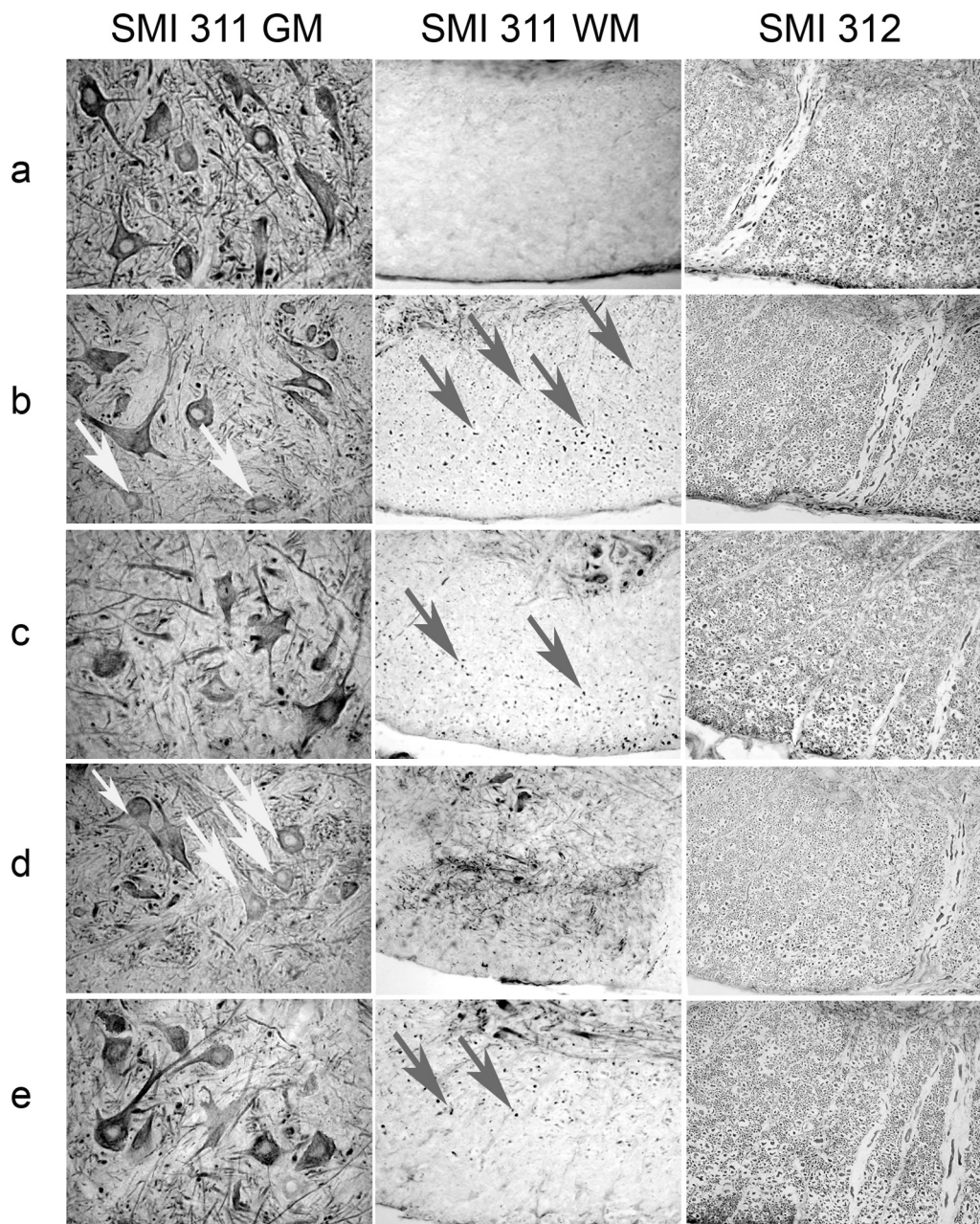
SMI 311 GM SMI 311 WM SMI 312

FIG. 4. AMPA receptor antagonist treatment reduces neuronal dysfunction, as observed by the phosphorylation state of heavy neurofilaments in mice infected with rOC/U$_{S241}$. Immunohistochemistry of lumbar spinal cord gray and white matter segments from mice infected with rOC/U$_{S241}$ or rOC/ATCC and treated with GYKI-52466 or vehicle at 10 dpi. In the normal spinal cord (a), SMI 311 stained the neurofilament of neuronal soma and dendrites. Following infection with rOC/ATCC or rOC/U$_{S241}$ (b or d, respectively), GM presented less SMI 311 neuronal soma staining, illustrating a loss of normal nonphosphorylated NF in GM compared to that for sham-infected mice (a), which was more pronounced following rOC/U$_{S241}$ infection than following rOC/ATCC infection (light arrows). Interestingly, spinal cord white matter of mice infected with rOC/ATCC (b) or rOC/U$_{S241}$ (d) showed higher levels of abnormal axonal nonphosphorylated NF-H, with abnormal axonal swelling, which was more pronounced following infection by rOC/U$_{S241}$ than following sham infection (a) (dark arrows). Staining with SMI 312 showed a low level of phosphorylated NF-H in WM axons following infection by rOC/U$_{S241}$ compared to that following rOC/ATCC or sham infection. GYKI-52466 treatment of mice infected with rOC/ATCC (c) or rOC/U$_{S241}$ (e) partially restored the physiological NF-H phosphorylation state. (a) Sham-infected mice plus vehicle; (b) rOC/ATCC-infected mice plus vehicle; (c) rOC/ATCC-infected mice plus GYKI-52466; (d) rOC/U$_{S241}$-infected mice plus vehicle; (e) rOC/U$_{S241}$-infected mice plus GYKI-52466. Magnification, ×400. Results are representative of two independent experiments with three mice per group.

U$_{S241}$ showed an abnormal presence of nonphosphorylated NF-H, and axonal swelling in WM was more important following rOC/U$_{S241}$ infection than following rOC/ATCC infection (Fig. 4, SMI 311 WM). Staining with SMI 312

antibodies against phosphorylated NF-H proteins showed a low level of axonal phosphorylated NF in the spinal cord white matter following infection by rOC/U$_{S241}$, compared to the level for rOC/ATCC- or sham-infected mice. Moreover,

GYKI-52466 treatment of mice infected by both recombinant viruses partially restored the physiological NF-H phosphorylation state.

GLT-1 expression is downregulated in mice infected by rOC/U$_{S241}$ and upregulated following AMPA receptor antagonist treatment. The astrocytic receptor GLT-1 is responsible for 90% of glutamate recapture. Consequently, as glutamate excitotoxicity may be due to a problem in this recapture, we decided to evaluate the expression of GLT-1 on spinal cord astrocytes. Spinal cords were harvested at 10 dpi, and GLT-1 expression was evaluated by immunofluorescence and Western blotting. Infection by both viruses led to significant astrocyte activation compared to that for sham-infected mice treated with vehicle (Fig. 5A and B) ($P < 0.001$). Even though a greater number of GFAP-positive astrocytes were detected following infection, glial GLT-1 expression was significantly downregulated in mice infected by rOC/U$_{S241}$ ($P < 0.01$), as revealed by immunofluorescence analysis (Fig. 5A) and confirmed by Western blotting (Fig. 5B), compared to levels in rOC/ATCC- and sham-infected mice. However, treatment with GYKI-52466 led to partial restoration of GLT-1 expression in mice infected by rOC/U$_{S241}$ ($P < 0.01$), as shown by immunofluorescence and Western blotting (Fig. 5A and B).

Treatment with AMPA receptor antagonist reduces microglial activation. Microglia are often activated during glutamate excitotoxicity. Therefore, microglial activation in the spinal cords of infected mice was evaluated by immunohistochemistry and Western blotting at 10 dpi. Mice infected by both viruses presented a significant activation of microglia/macrophages in the spinal cord, whereas in sham-infected mice, these cells were not activated under normal physiological conditions. Moreover, rOC/U$_{S241}$ infection led to a drastically significant increase ($P < 0.05$) in the activation of microglial cells compared to that seen with rOC/ATCC infection, as revealed by quantitation of Mac-2 expression on Western blots (Fig. 6A and B). Treatment with GYKI-52466 reduced activation of microglia/macrophages (Mac-2 expression) in mice infected with rOC/U$_{S241}$ ($P < 0.05$), but the level of microglial activation did not return to the basal level of sham-infected animals.

DISCUSSION

We have previously shown that four mutations in the spike (S) glycoprotein of HCoV-OC43 (D24Y, S83T, H183R, and Y241H) modulate disease in infected BALB/c mice from an encephalitis to a flaccid paralysis and eventual demyelination (24). The aim of the present study was to determine whether only one of these four mutations was sufficient to induce hindlimb paralysis in mice and to determine the mechanism underlying this virus-induced neuropathology. Making use of a series of recombinant viruses produced with our infectious clone pBAC-OC43^{FL} (47), we were able to identify a single point mutation (Y241H) in the HCoV-OC43 S glycoprotein that is necessary and sufficient for induction of hind-limb paralysis in infected BALB/c mice without affecting viral neurovirulence or the kinetics of viral replication in brain compared to those seen with rOC/ATCC.

Even though in some viral models of CNS infection, blockade of excitotoxicity results in a decrease in mortality of infected mice (21), we showed that treatment with an AMPA

antagonist affected neither the survival rate of mice nor the viral replication in mice infected by either HCoV-OC43 variant (rOC/ATCC or rOC/U$_{S241}$). However, the number of mice presenting motor dysfunctions or severe paralysis induced by the rOC/U$_{S241}$ variant decreased in the presence of the AMPA antagonist GYKI-52466, and mice recovered more rapidly from motor disability than infected mice treated with vehicle alone. These results strongly suggest that glutamate excitotoxicity is involved in the pathological process leading to motor dysfunction without any direct association with viral replication, which is not modified by the treatment with the AMPA antagonist.

Mice infected by rOC/U$_{S241}$ or rOC/ATCC showed abnormal loss of soma nonphosphorylated NF-H in the gray matter (GM), and this was more important following rOC/U$_{S241}$ infection. Moreover, spinal cord white matter (WM) of mice infected by rOC/U$_{S241}$ or rOC/ATCC presented abnormal axonal nonphosphorylated NF-H, which was also more important following rOC/U$_{S241}$ infection, even leading to axonal beading and swelling. It has already been reported that modifications in the phosphorylation state of neurofilaments contribute to motor neuron disease, as seen in amyotrophic lateral sclerosis (ALS) and multiple sclerosis (MS) (9, 43). This abnormal disruption of the NF-H phosphorylation state in the axon and cell body observed following infection could lead to neuronal dysfunction, i.e., disruption of axonal transport with perturbations in neuronal transmission, which has been demonstrated to account for motor disabilities (36). Treatment with GYKI-52466 significantly reduced the imbalance of the NF-H phosphorylation state and also improved motor dysfunctions. This is consistent with the fact that glutamate excitotoxicity causes damage to the cytoskeleton of axons *in vivo* and that the administration of AMPA antagonist attenuated axonal damages (18). Moreover, glutamate excitotoxicity was shown to be involved in the slowing of axonal transport (1, 22, 31), which could account for axonal swelling observed. As neurons are the main target of HCoV-OC43 infection, viral replication in neurons may induce neuronal stress that can lead to a dysregulation of glutamate metabolism and homeostasis (glutamate synthesis, release, recycling), as already shown in other neurotropic viral models (26, 33, 51). Indeed, it was reported that human immunodeficiency virus type 1 (HIV-1) can upregulate glutaminase expression in infected macrophages (15) and that the HIV-1 viral Tat protein increases neuronal glutamate exocytosis (32). Moreover, other studies have shown that the astrocytic glutamate transporter GLT-1 was downregulated in viral models involving Sindbis virus or HIV (11, 53). Furthermore, excessive stimulation of glutamate on its specific receptors is known to induce degeneration of neural cells and to lead to neurodegenerative diseases (13).

Under physiological conditions, glutamate homeostasis is regulated in large part by glial glutamate transporter 1 (GLT-1), expressed mainly on astrocytes, which is responsible for up to 90% of the total glutamate clearance in the adult CNS (2). We showed a significant activation of astrocytes following infection by both viruses. However, the expression of GLT-1 did not correlate with this activation being associated with an increased number of astrocytes expressing high levels of GFAP. Indeed, the results presented in Fig. 5 show that GLT-1 transporter expression was significantly downregulated following
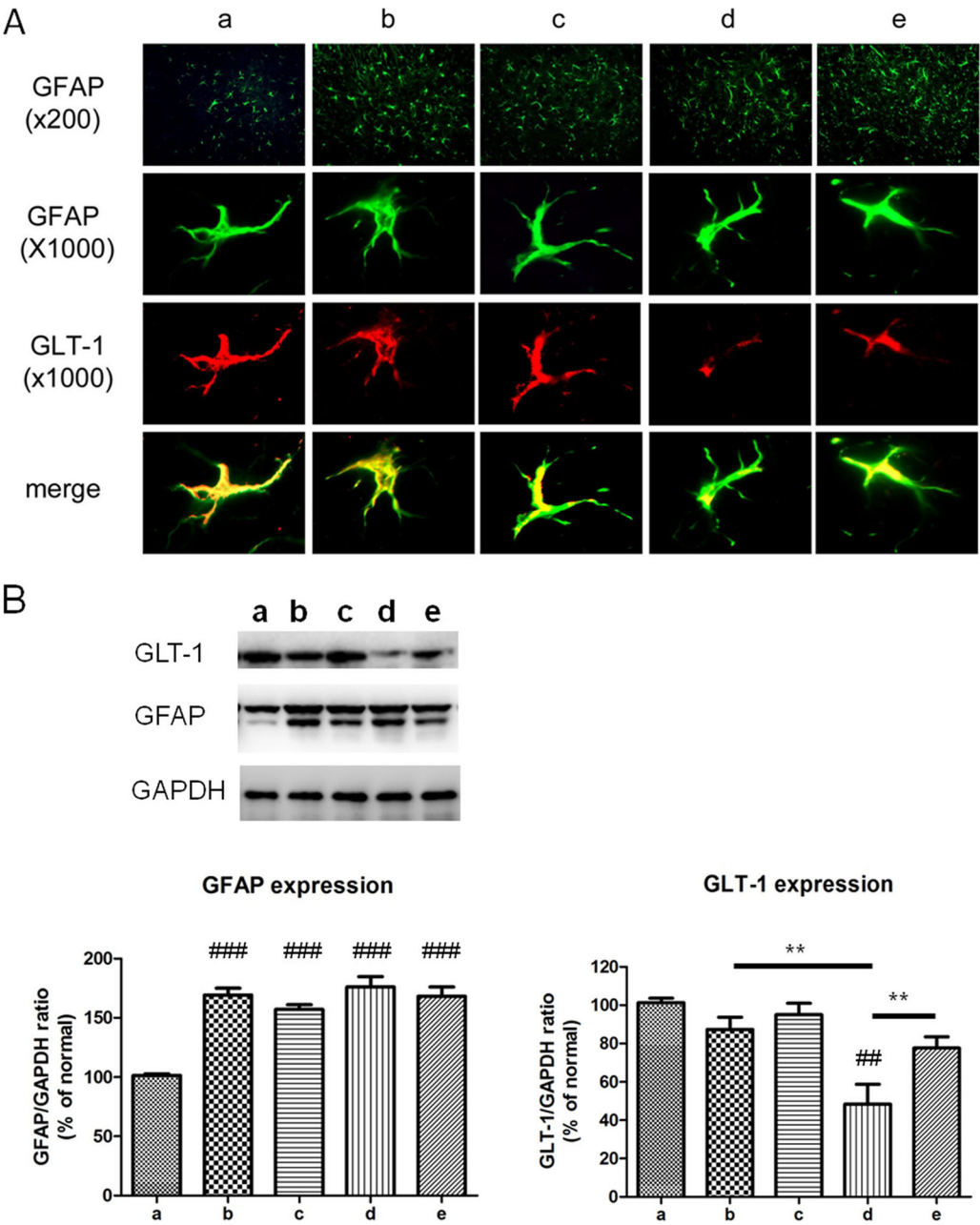
FIG. 5. Expression of GLT-1 is downregulated in mice infected with rOC/U$_{S241}$ and partially restored following treatment with AMPA receptor antagonist. (A) Immunofluorescence analysis of lumbar spinal cord segments of gray matter from mice infected by rOC/ATCC or rOC/U$_{S241}$ and treated with vehicle (b and d) or GYKI-52466 (c and e) at 10 dpi. Infected mice (b and d) presented an increased number of activated astrocytes compared to that seen with sham-infected mice (a), as well as a downregulation of GLT-1 staining which was more pronounced following rOC/U$_{S241}$ infection (d) than following rOC/ATCC infection (b). Treatment with GYKI-52466 led to partial restoration of GLT-1 expression levels (c and e). Results are representative of two independent experiments with three mice per group. (B) Western blotting strengthened histological data. Mice infected by both recombinants showed significant (###, $P < 0.001$) GFAP expression compared to that for sham-infected mice. GLT-1 expression was significantly downregulated in mice infected by rOC/U$_{S241}$ (d) (##, $P < 0.01$) compared to the level in mice infected by rOC/ATCC (b) or control (a). Treatment with GYKI-52466 led to significant upregulation of GLT-1 expression in mice infected by rOC/U$_{S241}$ (**, $P < 0.01$) compared to that in mice infected by rOC/ATCC or control. Note that following infection of mice with HCoV-OC43, an additional band of GFAP is detected at 45 kDa, which is suggested to represent a proteolytic fragment derived from the 50-kDa band. Results are expressed as percentages of control (sham-infected mice plus vehicle [a]), and data are represented as means ± SEM ($n = 3$). (a) Sham-infected mice plus vehicle; (b) rOC/ATCC-infected mice plus vehicle; (c) rOC/ATCC-infected mice plus GYKI-52466; (d) rOC/U$_{S241}$-infected mice plus vehicle; (e) rOC/U$_{S241}$-infected mice plus GYKI-52466. Results are representative of three independent experiments.
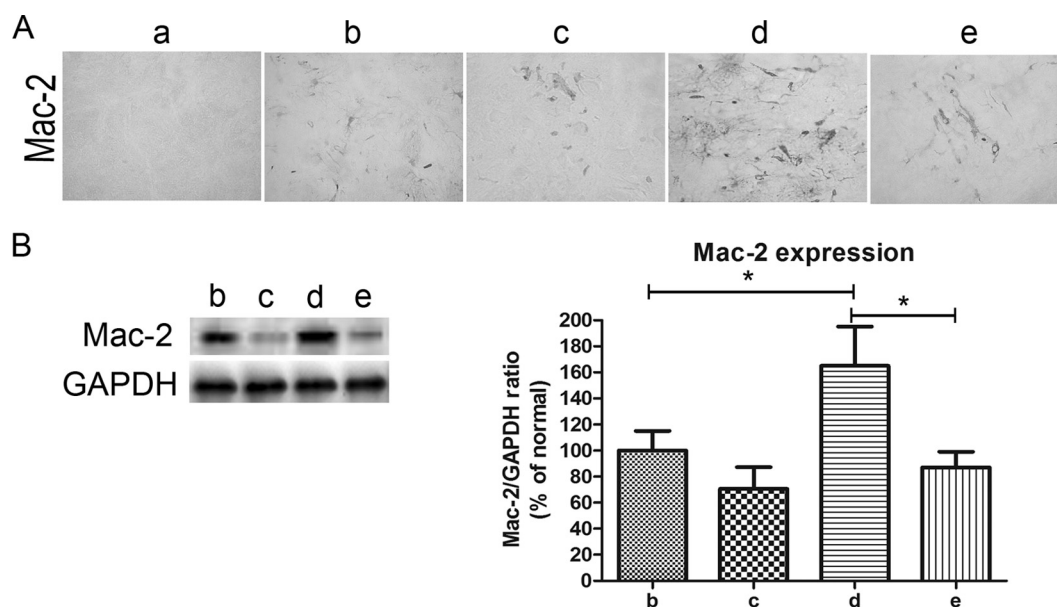
FIG. 6. Treatment with AMPA receptor antagonist reduced microglial activation. (A) Immunohistochemical staining of activated microglia, using Mac-2 antibody in mice infected with rOC/U_{S241} or rOC/ATCC and treated with GYKI-52466 or vehicle at 10 dpi. The spinal cord gray matter ventral horn from infected mice demonstrated a significant activation of microglia/macrophages following infection by both viruses. Treatment with GYKI-52466 reduced microglia/macrophage activation in mice infected by rOC/U_{S241}. Magnification, ×400. Results are representative of two independent experiments with three mice per group. (B) Western blotting of spinal cord proteins confirmed the histological finding. Infection of mice by rOC/U_{S241} led to significant ($*$, $P < 0.05$) increased activation of microglial cells (Mac-2 staining) compared to that in mice infected by rOC/ATCC, and GYKI-52466 treatment attenuated microglial cell activation in mice infected by rOC/U_{S241} ($*$, $P < 0.05$). These results are expressed as percentages of the reference value, with 100% representing mice infected by rOC/ATCC and treated with vehicle (b), as microglial cell activation was undetectable in sham-infected animals (a). Data are represented as means ± SEM ($n = 3$). (a) Sham-infected mice plus vehicle; (b) rOC/ATCC-infected mice plus vehicle; (c) rOC/ATCC-infected mice plus GYKI-52466; (d) rOC/U_{S241}-infected mice plus vehicle; (e) rOC/U_{S241}-infected mice plus GYKI-52466. Results are representative of three independent experiments.

rOC/U_{S241} infection compared to that following rOC/ATCC or sham infection. Interestingly, treatment with GYKI-52466 led to a partial restoration of expression of the GLT-1 transporter, although expression always remained inferior to basal levels. This incomplete restoration may account for the remaining motor dysfunctions observed. It was demonstrated that GLT-1 knockout mice undergo seizures and death as a result of excitotoxicity caused by too-elevated extracellular glutamate concentrations (50). Moreover, decreased expression of this transporter has been reported in several neurological diseases, as well as in viral models (7, 17).

We have previously reported that infection of mice by HCoV-OC43 led to the release of several proinflammatory cytokines (tumor necrosis factor alpha [TNF-α], interleukin-1 [IL-1], and IL-6), with a significant increase of IL-6 in mice infected with an S mutant virus (24). These cytokines are known to downregulate glutamate transporter GLT-1 expression (11, 34, 38). In the present study, we show that the mutant virus rOC/U_{S241} (which harbors a single S point mutation, Y241H) led to significant microglia/macrophage activation compared to what is observed with the reference virus and that treatment with the AMPA antagonist partially reduced microglial cell activation. Moreover, our results (Fig. 6) also indicate that the increased microglia/macrophage activation correlated with the GLT-1 downregulated expression. Previous studies have demonstrated that microglia/macrophages can sense extracellular glutamate concentration via AMPA receptors on their membrane and that glutamate acts as a chemokine for

these cells (29). Furthermore, activated microglia/macrophages are a significant source of glutamate that can induce excitotoxic neuronal cell death (6). These results suggest that, in our model, the role of astrocytes is to rescue neurons from excitotoxicity by regulating glutamate homeostasis, whereas activation of microglia/macrophages may exert excitotoxicity by downregulating GLT-1 expression via the release of some cytokines or by releasing glutamate, as previously described (28). This is consistent with a previous study that showed that microglia/macrophages can release glutamate and that blockade of glutamate release from activated microglia attenuates experimental autoimmune encephalomyelitis in mice (45).

In summary, our study suggests that persistence-acquired mutations in the S glycoprotein of a human coronavirus (HCoV-OC43), which represents a possible viral adaptation within the CNS, could be involved in the development of neurological disorders in humans and that a single such point mutation is sufficient to modulate virus-induced neuropathology from an encephalitis to an MS-like neuropathology that involves glutamate excitotoxicity in a mouse model. Deciphering the underlying mechanisms of HCoV-OC43 interaction with the central nervous system should lead to a better understanding of potentially pathological consequences of this infection, as well as the importance of viral determinants in the process. Future studies will investigate the mechanism of action of both viruses (rOC/ATCC and rOC/U_{S241}) regarding glutamate synthesis, release, and uptake in order to better

understand the exact role of excitotoxicity and its pathological consequences following HCoV-OC43 infection.

REFERENCES

1. **Ackerley, S., et al.** 2000. Glutamate slows axonal transport of neurofilaments in transfected neurons. J. Cell Biol. **150:**165–176.
2. **Anderson, C. M., and R. A. Swanson.** 2000. Astrocyte glutamate transport: review of properties, regulation, and physiological functions. Glia **32:**1–14.
3. **Arbour, N., et al.** 1999. Acute and persistent infection of human neural cell lines by human coronavirus OC43. J. Virol. **73:**3338–3350.
4. **Arbour, N., R. Day, J. Newcombe, and P. J. Talbot.** 2000. Neuroinvasion by human respiratory coronaviruses. J. Virol. **74:**8913–8921.
5. **Arbour, N., et al.** 1999. Persistent infection of human oligodendrocytic and neuroglial cell lines by human coronavirus 229E. J. Virol. **73:**3326–3337.
6. **Barger, S. W., M. E. Goodwin, M. M. Porter, and M. L. Beggs.** 2007. Glutamate release from activated microglia requires the oxidative burst and lipid peroxidation. J. Neurochem. **101:**1205–1213.
7. **Blakely, P. K., B. K. Kleinschmidt-DeMasters, K. L. Tyler, and D. N. Irani.** 2009. Disrupted glutamate transporter expression in the spinal cord with acute flaccid paralysis caused by West Nile virus infection. J. Neuropathol. Exp. Neurol. **68:**1061–1072.
8. **Bonavia, A., N. Arbour, V. W. Yong, and P. J. Talbot.** 1997. Infection of primary cultures of human neural cells by human coronaviruses 229E and OC43. J. Virol. **71:**800–806.
9. **Boylan, K., et al.** 2009. Immunoreactivity of the phosphorylated axonal neurofilament H subunit (pNF-H) in blood of ALS model rodents and ALS patients: evaluation of blood pNF-H as a potential ALS biomarker. J. Neurochem. **111:**1182–1191.
10. **Buchmeier, M. J., and T. E. Lane.** 1999. Viral-induced neurodegenerative disease. Curr. Opin. Microbiol. **2:**398–402.
11. **Carmen, J., J. D. Rothstein, and D. A. Kerr.** 2009. Tumor necrosis factor-alpha modulates glutamate transport in the CNS and is a critical determinant of outcome from viral encephalomyelitis. Brain Res. **1263:**143–154.
12. **Danbolt, N. C.** 2001. Glutamate uptake. Prog. Neurobiol. **65:**1–105.
13. **Dong, X. X., Y. Wang, and Z. H. Qin.** 2009. Molecular mechanisms of excitotoxicity and their relevance to pathogenesis of neurodegenerative diseases. Acta Pharmacol. Sin. **30:**379–387.
14. **Edwards, J. A., F. Denis, and P. J. Talbot.** 2000. Activation of glial cells by human coronavirus OC43 infection. J. Neuroimmunol. **108:**73–81.
15. **Erdmann, N., et al.** 2009. *In vitro* glutaminase regulation and mechanisms of glutamate generation in HIV-1 infected macrophages. J. Neurochem. **109:**551–561.
16. **Forgie, S., and T. J. Marrie.** 2009. Healthcare-associated atypical pneumonia. Semin. Respir. Crit. Care Med. **30:**67–85.
17. **Fotheringham, J., E. L. Williams, N. Akhyani, and S. Jacobson.** 2008. Human herpesvirus 6 (HHV-6) induces dysregulation of glutamate uptake and transporter expression in astrocytes. J. Neuroimmune Pharmacol. **3:**105–116.
18. **Fowler, J. H., E. McCracken, D. Dewar, and J. McCulloch.** 2003. Intracerebral injection of AMPA causes axonal damage in vivo. Brain Res. **991:**104–112.
19. **Gotow, T.** 2000. Neurofilaments in health and disease. Med. Electron Microsc. **33:**173–199.
20. **Goulton, C. S., A. R. Patten, J. R. Kerr, and D. S. Kerr.** 2010. Pharmacological preconditioning with GYKI 52466: a prophylactic approach to neuroprotection. Front. Neurosci. **4:**54.
21. **Greene, I. P., E. Y. Lee, N. Prow, B. Ngwang, and D. E. Griffin.** 2008. Protection from fatal viral encephalomyelitis: AMPA receptor antagonists have a direct effect on the inflammatory response to infection. Proc. Natl. Acad. Sci. U. S. A. **105:**3575–3580.
22. **Hiruma, H., T. Katakura, S. Takahashi, T. Ichikawa, and T. Kawakami.** 2003. Glutamate and amyloid beta-protein rapidly inhibit fast axonal transport in cultured rat hippocampal neurons by different mechanisms. J. Neurosci. **23:**8967–8977.
23. **Jacomy, H., G. Fragoso, G. Almazan, W. E. Mushynski, and P. J. Talbot.** 2006. Human coronavirus OC43 infection induces chronic encephalitis leading to disabilities in BALB/C mice. Virology **349:**335–346.
24. **Jacomy, H., et al.** 2010. Mutations in the spike glycoprotein of human coronavirus OC43 modulate disease in BALB/c mice from encephalitis to flaccid paralysis and demyelination. J. Neurovirol. **16:**279–293.
25. **Jacomy, H., and P. J. Talbot.** 2003. Vacuolating encephalitis in mice infected by human coronavirus OC43. Virology **315:**20–33.
26. **Kaul, M., G. A. Garden, and S. A. Lipton.** 2001. Pathways to neuronal injury and apoptosis in HIV-associated dementia. Nature **410:**988–994.
27. **Lambert, F., H. Jacomy, G. Marceau, and P. J. Talbot.** 2008. Titration of human coronaviruses, HCoV-229E and HCoV-OC43, by an indirect immunoperoxidase assay. Methods Mol. Biol. **454:**93–102.
28. **Liang, J., et al.** 2008. Excitatory amino acid transporter expression by astrocytes is neuroprotective against microglial excitotoxicity. Brain Res. **1210:** 11–19.
29. **Liu, G. J., R. Nagarajah, R. B. Banati, and M. R. Bennett.** 2009. Glutamate induces directed chemotaxis of microglia. Eur. J. Neurosci. **29:**1108–1118.
30. **Mark, L. P., et al.** 2001. Pictorial review of glutamate excitotoxicity: fundamental concepts for neuroimaging. Am. J. Neuroradiol. **22:**1813–1824.
31. **Miller, C. C., et al.** 2002. Axonal transport of neurofilaments in normal and disease states. Cell. Mol. Life Sci. **59:**323–330.
32. **Musante, V., et al.** 2010. The HIV-1 viral protein Tat increases glutamate and decreases GABA exocytosis from human and mouse neocortical nerve endings. Cereb. Cortex **20:**1974–1984.
33. **Nargi-Aizenman, J. L., and D. E. Griffin.** 2001. Sindbis virus-induced neuronal death is both necrotic and apoptotic and is ameliorated by N-methyl-D-aspartate receptor antagonists. J. Virol. **75:**7114–7121.
34. **Okada, K., U. Yamashita, and S. Tsuji.** 2005. Modulation of Na(+)-dependent glutamate transporter of murine astrocytes by inflammatory mediators. J. UOEH **27:**161–170.
35. **Olney, J. W.** 1978. Neurotoxicity of excitatory amino acids, p. 95–121. *In* E. G. McGeer, J. W. Olney, and P. L. McGeer (ed.), Kainic acid as a tool in neurobiology. Raven Press, New York, NY.
36. **Perrot, R., R. Berges, A. Bocquet, and J. Eyer.** 2008. Review of the multiple aspects of neurofilament functions, and their possible contribution to neurodegeneration. Mol. Neurobiol. **38:**27–65.
37. **Petzold, A.** 2005. Neurofilament phosphoforms: surrogate markers for axonal injury, degeneration and loss. J. Neurol. Sci. **233:**183–198.
38. **Prow, N. A., and D. N. Irani.** 2008. The inflammatory cytokine, interleukin-1 beta, mediates loss of astroglial glutamate transport and drives excitotoxic motor neuron injury in the spinal cord during acute viral encephalomyelitis. J. Neurochem. **105:**1276–1286.
39. **Riski, H., and T. Hovi.** 1980. Coronavirus infections of man associated with diseases other than the common cold. J. Med. Virol. **6:**259–265.
40. **Rorick-Kehn, L. M., J. C. Hart, and D. L. McKinzie.** 2005. Pharmacological characterization of stress-induced hyperthermia in DBA/2 mice using metabotropic and ionotropic glutamate receptor ligands. Psychopharmacology **183:**226–240.
41. **Rota, P. A., et al.** 2003. Characterization of a novel coronavirus associated with severe acute respiratory syndrome. Science **300:**1394–1399.
42. **Sattler, R., and M. Tymianski.** 2000. Molecular mechanisms of calcium-dependent excitotoxicity. J. Mol. Med. **78:**3–13.
43. **Schirmer, L., J. P. Antel, W. Bruck, and C. Stadelmann.** 2011. Axonal loss and neurofilament phosphorylation changes accompany lesion development and clinical progression in multiple sclerosis. Brain Pathol. **21:**428–440.
44. **Shea, T. B., W. K. Chan, J. Kushkuley, and S. Lee.** 2009. Organizational dynamics, functions, and pathobiological dysfunctions of neurofilaments. Results Probl. Cell Differ. **48:**29–45.
45. **Shijie, J., et al.** 2009. Blockade of glutamate release from microglia attenuates experimental autoimmune encephalomyelitis in mice. Tohoku J. Exp. Med. **217:**87–92.
46. **Solyom, S., and I. Tarnawa.** 2002. Non-competitive AMPA antagonist of 2,3-benzodiazepine type. Curr. Pharm. Des. **8:**913–939.
47. **St-Jean, J. R., et al.** 2006. Recovery of a neurovirulent human coronavirus OC43 from an infectious cDNA clone. J. Virol. **80:**3670–3674.
48. **St-Jean, J. R., M. Desforges, and P. J. Talbot.** 2006. Genetic evolution of human coronavirus OC43 in neural cell culture. Adv. Exp. Med. Biol. **581:** 499–502.
49. **Talbot, P. J., H. Jacomy, and M. Desforges.** 2008. Pathogenesis of human coronaviruses other than severe acute respiratory syndrome coronavirus, p. 313–324. *In* S. Perlman, T. Gallagher, and E. J. Snijder (ed.), Nidoviruses. ASM Press, Washington, DC.
50. **Tanaka, K., et al.** 1997. Epilepsy and exacerbation of brain injury in mice lacking the glutamate transporter GLT-1. Science **276:**1699–1702.
51. **Tian, C., et al.** 2008. HIV-infected macrophages mediate neuronal apoptosis through mitochondrial glutaminase. J. Neurochem. **105:**994–1005.
52. **Tilleux, S., and E. Hermans.** 2007. Neuroinflammation and regulation of glial glutamate uptake in neurological disorders. J. Neurosci. Res. **85:**2059–2070.
53. **Wang, Z., et al.** 2003. Reduced expression of glutamate transporter EAAT2 and impaired glutamate transport in human primary astrocytes exposed to HIV-1 or gp120. Virology **312:**60–73.
54. **Yeh, E. A., A. Collins, M. E. Cohen, P. K. Duffner, and H. Faden.** 2004. Detection of coronavirus in the central nervous system of a child with acute disseminated encephalomyelitis. Pediatrics **113:**e73–e76.